Published by
NIGERIAN SOCIETY OF PHYSICAL SCIENCES
Available online @ https://journal.nsps.org.ng/index.php/jnsps

J. Nig. Soc. Phys. Sci. 5 (2023) 1435

Journal of the Nigerian Society of Physical Sciences

Numerical investigation of nonlinear radiative flux of non-Newtonian MHD fluid induced by nonlinear driven multi-physical curved mechanism with variable magnetic field

K. M. Sanni[a,*], A. D. Adeshola[b], T. O. Aliu[b]

[a]*Department of Mathematics, COMSATS University Islamabad, Chak Shahzad Road, Islamabad, 44000*
[b]*Department of Mathematics and Statistics, Kwara State University Malete*

Abstract

This paper discusses two-dimensional heat flow of an incompressible non-Newtonian hydromagnetic fluid over a power-law stretching curved sheet. The energy equation of the flow problem considers a radiative flux influenced by viscous dissipation and surface frictional heating. Lorentz force and Joule heating are taken in the consequence of applied variable magnetic field satisfying solenoidal nature of magnetism. The governing equations are reduced to boundary-layer regime using dimensionless quantities and the resulting PDEs are converted into ODEs by suitable similarity variables. The flow fields; velocity and temperature are computed numerically by implementing Keller-Box shooting method with Jacobi iterative technique. Error analysis is calculated to ensure solutions' convergence. Interesting flow parameters are examined and plotted graphically. Results show that velocity is increased for large number of fluid rheology and opposite effects are recorded for increasing curvature, Lorentz force, and stretching power. Flow past a flat and curved surfaces are substantial in validation of this present work.

DOI:10.46481/jnsps.2023.1435

Keywords: Power-law, cross fluid, radiation, dissipation, MHD, curved surface, Joule heating.

Article History :
Received: 01 March 2023
Received in revised form: 09 May 2023
Accepted for publication: 10 May 2023
Published: 29 May 2023

© 2023 The Author(s). Published by the Nigerian Society of Physical Sciences under the terms of the Creative Commons Attribution 4.0 International license (*https://creativecommons.org/licenses/by/4.0*). Further distribution of this work must maintain attribution to the author(s) and the published article's title, journal citation, and DOI.

Communicated by: O. Adeyeye

1. Introduction

Several studies that addressed heat transfer problems in thermal engineering have been documented over the years. Attentions have been given towards heat flow and thermal energy exchange through a physical system that involve heat mechanisms like convection, conduction as well as radiation. This is due to undisputed applications of heat generation, heat conversions, and heat transfer of energy by phase changes in various devices including condensers, boilers, and evaporators. However, fluids flow accompanied by thermal energy over stretchable materials have important applications in many industrial processes which are not limited to- cooling of metallic sheets, liquified and plastic film, glass blowing, paper production, drawing of plastic film, glass fiber, food processing, polymer sheet extrusion from dye among several others. Nevertheless, evolution of boundary-layer study of heat transfer for non-Newtonian fluids tremendously plays a vital role in processing of material and manufacturing products. Non-Newtonian fluids have been extensively investigated in account for the dynamic behaviours of most natural, biological, and industrial fluids.

*Corresponding author tel. no:
Email address: annikennie13@gmail.com (K. M. Sanni)

So far there is no unique model that exhibits all the characteristics of non-Newtonian fluids. In response to this observation, various rheology models have been established with certain precisions and limitations. Nonlinear stretching terms such as power-law, exponential, and quadratic have extensively examined to have greater impacts on flow problems physically in view of real-life scenarios. These forms of stretching exhibition are more challenging in exploring the physical significance of flow situations. Literature on this subject is so enormous to be discussed here hence, the present investigation concentrates only on recent published articles. Hayat *et al.* [1] examined the heat transport influenced by Cattaneo-Christov heat flux of a stagnation point flow induced past a nonlinear stretching surface. They concluded that non-Fourier heat flux reduces the heat flow as compared with Fourier expression. Rout and Mishra [2] discussed the heat transfer of a hydromagnetic nanofluid over an unsteady stretching surface.

Turkyilmazoglu [3] investigated heat transfer of a micropolar fluid flow past a stretching porous sheet. He presented a unique close form solution which satisfied the entire physical parameters of the problem. Zeeshan *et al.* [4] documented the flow of viscous ferro-fluid induced by a stretching surface with magnetic dipole effect and thermal radiation. Their results showed that increased magnetic parameter diminished the velocity field and enhanced the temperature distribution. The numerical solution of Carreau nanofluid flow induced by a nonlinear stretching porous surface is carried out by Mohamed *et al.* [5] in which the impact of rheology parameter of the fluid showed kinetic differences between pseudo-plastic and dilatant nanofluid. Prasnnakumara *et al.* [6] examined the flow of MHD Sisko nanofluid with nonlinear radiation over nonlinear stretching sheet whereas collocation method is applied by Feroz et a. [7] to analyze the melting heat of Sisko fluid past a moving sheet.

Lund *et al.* [8] investigated dual solution of hydromagnetic Williamson fluid flow with slip condition. Khalil *et al.* [9] presented a numerical treatment of MHD Casson fluid flow with thermal stratification and dual convection. The heat transport of MHD power-law fluid by virtue of Lie-group analysis is provided by Mohamed *et al.* [10]. Hayat *et al.* [11] carried out numerical simulation of MHD Cross fluid past a stagnation point stretching flat sheet with energy equation under certain flow conditions. Khan *et al.* [12] examined heat flow of a Cross fluid along axisymmetric channel in a radially stretched plate. Effects of mixed convection and thermal radiative heat flux of a Cross fluid over a stretching plane surface are investigated by Manzur *et al.* [13]. For more relevant studies for non-Newtonian fluids in the light of Ellis fluid, Eyring-Powell fluid, Maxwell fluid, Sutterby fluid, second and third grade fluids, and etc., interested readers are referred [14-26].

The fluid flow induced by curved stretching sheet has attracted the interest of researchers in the last decade because of its applications in engineering of stretchable curved materials. Initiated by the fundamental paper of Sajid *et al.* [27], Abbas *et al.* [28] included heat transfer analysis in an electrically conducting Newtonian fluid flow over stretching curved surface. The results provided in these articles have been recently revised by Sanni *et al.* [29, 30] with the accurate magnetic field included in the momentum equations. The results are modified having satisfied solenoidal magnetic property, $\nabla.\mathbf{B} = \mathbf{0}$, as well as the geometry. The consequences of internal heat generation in a flow of nanofluid induced by stretched curved surface is studied by Saba *et al.* [31]. Hayat *et al.* [32] offered the impacts of homogeneous-heterogeneous reaction on electrically conducting Micropolar fluid past a curved stretching sheet whereas in an unsteady permeable curved sheet, Saleh *et al.* [33] analyzed the shrinking and stretching flow scenario.

The flow of MHD viscous fluid is documented by Naveed *et al.* [34] under dual solution effects with shrinking curved sheet likewise Sanni *et al.* [35] documented the viscous fluid flow caused by a nonlinear power-law driven curved surface. Nadeem *et al.* [36] worked on magneto nanofluid over a stretching curved surface in the presence of variable viscosity and carbon nanotubes. Studies from the aforementioned literature revealed that absolutely, no investigation of heat transport of non-Newtonian Cross fluid over a power-law stretching curved surface has been addressed. Therefore, the prime objective of this study is to investigate heat transfer of a Cross fluid under certain flow conditions. It is worth mentioning that non-Newtonian rheological model of some fluids like Sisko fluid, Bingham fluid, and power-law fluid can be recovered with definite constraints being met from Cross fluid viscosity equation. For instance, it turns Sisko model if $\xi \ll \xi_0$, Bingham model taking $n = 1$, and power-law model for $\xi \ll \xi_0$ and $\xi \gg \xi_\infty$ [37].

Characterizing parameters, n and Γ, of the fluid curve fitting are more important due to strong flow prediction at low and high shear rates. In addition, applied variable magnetic field is considered due to solenoidal nature of magnetism and to elucidates its consequences on the Lorentz force and surface frictional heating. This work is prepared in sections that is the basic equations for the flow momentum, problem description accompanied by the heat transport, numerical computations, and results and discussion. Special cases of Newtonian fluid for flat and curved surfaces remain vital to authenticate the present findings. The results obtained are significantly useful in thermal engineering and manufacturing processing of stretchable sheets.

2. Model Description

Consider rheological Cross fluid model and Navier-Stokes equation of an incompressible fluid with body force as [37]:

$$\overline{S} = \eta_\infty + (\eta_0 - \eta_\infty)\left[\frac{1}{1 + (\Gamma\dot{\gamma})^n}\right]\mathbf{A_1}, \tag{1}$$

$$\rho\frac{D\overline{V}}{Dt} = -\overline{p} + \overline{\nabla}.\overline{S} + \overline{F}, \tag{2}$$

$$\overline{\nabla}.\overline{V} = 0, \tag{3}$$

where $\overline{S}$ is the extra stress tensor with η_0 and η_∞ being low and infinite shear viscosity shear rate, n, Γ, and $\dot{\gamma} = \sqrt{\frac{trace(A_1)^2}{2}}$

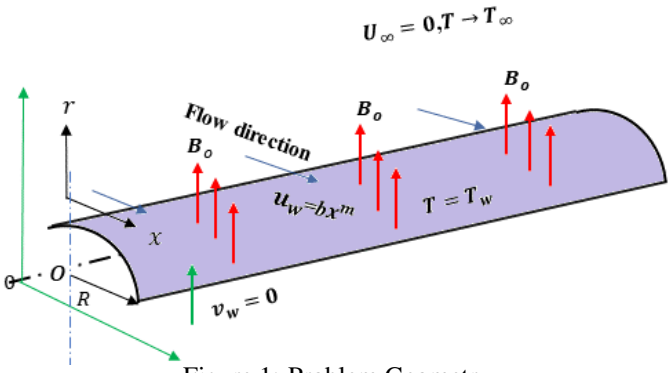


Figure 1: Problem Geometry

represent fluid behavioural index, material constant, and strain rate tensor respectively. Fluid density denoted by ρ, velocity field $\overline{V} = (v, u, 0)$, p symbolizes the pressure, $\overline{F}$ the body force, and $\overline{\nabla} = \hat{e_r}\frac{\partial}{\partial r} + \hat{e_s}\frac{R}{R+r}\frac{\partial}{\partial s}$, in which $\hat{e_r}$ and $\hat{e_s}$ are unit vector in radial, $r-$ and axial, $s-$ directions. Presenting 2D curvilinear coordinates system $(r, s, 0)$, the first Rivlin-Erickson tensor $\mathbf{A_1} = \overline{\nabla}\overline{\mathbf{V}} + (\overline{\nabla}\overline{\mathbf{V}})^{\mathbf{T}}$ is given by

$$A_1 = \begin{bmatrix} 2\frac{\partial v}{\partial r} & \frac{\partial u}{\partial r} + \frac{R}{R+r}\frac{\partial v}{\partial s} - \frac{u}{R+r} \\ \frac{\partial u}{\partial r} + \frac{R}{R+r}\frac{\partial v}{\partial s} - \frac{u}{R+r} & \frac{2R}{R+r}\frac{\partial u}{\partial s} + \frac{2v}{R+r} \end{bmatrix}. \tag{4}$$

3. Problem Formulation

The steady 2D flow of an incompressible electrically conducting fluid driven by nonlinear curved stretching sheet of radius R is considered. The magnetic field $\overline{B}(r) = \frac{RB_0}{R+r}\hat{e}_r$ is variably imposed satisfying the solenoidal magnetic property and perpendicular to flow direction. A resistive force under the effect of magnetic Reynolds number yields $\overline{F} = \overline{J} \times \overline{B}$. Electrical field varnishes as $E \approx 0$ induced a negligible magnetic field implying that the current density $\overline{J} = \sigma(\overline{V} \times \overline{B})$. Then we get

$$\bar{\mathbf{F}} = (-\sigma\frac{\mathbf{RB_0}}{\mathbf{r}+\mathbf{R}}\mathbf{u}, \mathbf{0}, \mathbf{0}), \tag{5}$$

where $\mathbf{B}_0$ is the strength of magnetic field and σ gives conductivity of the fluid. Physical problem geometry is represented in Fig. 1. Utilizing Eqs. (1) - (5), governing flow equations can be expressed as following

$$\frac{\partial v}{\partial r} + \frac{R}{r+R}\frac{\partial u}{\partial s} + \frac{v}{r+R} = 0 \tag{6}$$

$$\begin{aligned} &v\frac{\partial v}{\partial r} + \frac{Ru}{R+r}\frac{\partial v}{\partial s} - \frac{u^2}{r+R} = -\frac{1}{\rho}\frac{\partial p}{\partial r} \\ &-N_1\left[S_{rs}\frac{\partial}{\partial r}\left(\frac{1}{1+(\Gamma\dot{\gamma})^n}\right) + \frac{RS_{ss}}{R+r}\frac{\partial}{\partial s}\left(\frac{1}{1+(\Gamma\dot{\gamma})^n}\right)\right] \\ &+N_2\left[\frac{1}{R+r}\frac{\partial}{\partial r}\left(\frac{RS_{rr}}{R+r}\right) + \frac{R}{R+r}\frac{\partial S_{rs}}{\partial s} - \frac{S_{ss}}{R+r}\right] \end{aligned} \tag{7}$$

$$\begin{aligned} &v\frac{\partial u}{\partial r} + \frac{Ru}{R+r}\frac{\partial u}{\partial s} + \frac{uv}{r+R} = -\frac{R}{\rho(R+r)}\frac{\partial p}{\partial s} \\ &-N_1\left[S_{rr}\frac{\partial}{\partial r}\left(\frac{1}{1+(\Gamma\dot{\gamma})^n}\right) + \frac{RS_{sr}}{R+r}\frac{\partial}{\partial s}\left(\frac{1}{1+(\Gamma\dot{\gamma})^n}\right)\right] \\ &+N_2\left[\frac{1}{R+r}\frac{\partial}{\partial r}\left(\frac{RS_{sr}}{R+r}\right) + \frac{R}{R+r}\frac{\partial S_{ss}}{\partial s} + \frac{S_{sr}}{R+r}\right] \\ &-\frac{\sigma R^2 B_o^2}{\rho(R+r)^2}u, \end{aligned} \tag{8}$$

such that $N_1 = \Gamma^n\frac{\eta_0 n}{2\rho}(\dot{\gamma})^{\frac{n-2}{2}}$ and $N_2 = \frac{\eta_0}{\rho}(1 - \Gamma^n(\dot{\gamma})^{\frac{n}{2}})$.

The corresponding stress components S_{rr}, S_{rs}, and S_{ss} are given as

$$S_{rr} = 2\frac{\partial v}{\partial r} \tag{9}$$

$$S_{rs} = \frac{\partial u}{\partial r} + \frac{R}{R+r}\frac{\partial v}{\partial s} - \frac{u}{R+r} \tag{10}$$

$$S_{ss} = \frac{2R}{R+r}\frac{\partial u}{\partial s} + \frac{2v}{R+r}. \tag{11}$$

Relevant boundary conditions associate with this problem are

$$u(0)|_{r=0} = as^m, v(0)|_{r=0} = 0, \tag{12}$$

$$u(\infty)|_{r\to\infty} = 0, \frac{\partial u(\infty)}{\partial r}|_{r\to\infty} = 0, \tag{13}$$

in which a is a constant $(l^{1-m}t^{-1})$ with l being the surface length, and m the stretching power. Employing suitable scale together with dimensionless characteristics of the form

$$\begin{aligned} &u^* = \frac{u}{U_\infty}, v^* = \frac{vl}{U_\infty\delta}, s^* = \frac{s}{l}, r^* = \frac{r}{\delta}, R^* = \frac{R}{\delta}, \\ &p^* = \frac{P}{\rho u_w^2}, b = \frac{\eta_0 n U_\infty^{2n}}{\delta^{2n}}. \end{aligned} \tag{14}$$

After using Eq. (14), Eqs (6)-(8) give the boundary-layer equations as

$$\frac{u^2}{r+R} = \frac{\partial P}{\partial r}, \tag{15}$$

$$\begin{aligned} &v\frac{\partial u}{\partial r} + \frac{Ru}{R+r}\frac{\partial u}{\partial s} + \frac{uv}{R+r} = -\frac{1}{\rho} - \frac{\sigma R^2 B_0^2}{\rho(R+r)^2}u, \\ &-N_3\left((n+1)\frac{\partial^2 u}{\partial r^2} - \frac{n-1}{R+r}\frac{\partial u}{\partial r} + \frac{n-1}{(R+r)^2}u\right) \\ &+\frac{\eta_0}{\rho}\left(\frac{\partial^2 u}{\partial r^2} + \frac{1}{R+r}\frac{\partial u}{\partial r} - \frac{u}{(r+R)^2}\right), \end{aligned} \tag{16}$$

in which $N_3 = nb\Gamma^n\left(\frac{\partial u}{\partial r} - \frac{u}{R+r}\right)^n$ whereas Eq. (6) is identically satisfied.

Existing models of Newtonian fluid for both flat and curved surface are recovered in the limiting state as $R \longrightarrow \infty$ at zeroth pressure, $P = 0$ and material constant $\Gamma = 0$ (see refs. 20,21,27).

Relevant similarity variables are calculated as follow

$$u = as^m h'(\xi), \xi^2 = r^2\frac{a\rho s^{(m-1)}}{\eta_0}, P = a^2 s^2 N(\xi), \tag{17}$$

$$\gamma^2 = R\frac{a\rho s^{(m-1)}}{\eta_0}, M^2 = \frac{\sigma B_0^2 a^2}{\eta_0}, Re_s = \frac{a\rho s^{(m+1)}}{\eta_0}, \tag{18}$$

$$v = -a\frac{R}{R+r}\sqrt{\frac{\eta_0 s^{(m-1)}}{\rho a}}\left[\left(\frac{m+1}{2}\right)h(\xi) + \xi\left(\frac{m-1}{2}\right)h'(\xi)\right], \quad (19)$$

where $h(\eta)$ denotes the flow stream, $h'(\eta)$ represents the flow speed, Re_s the Reynolds number, and U_∞ the ambient velocity. By virtue of Eqs. (17)-(19), Eqs. (15) and (16) become

$$\frac{(h')^2}{\xi+\gamma} = N'(\xi) \quad (20)$$

$$\begin{aligned}\frac{2m\gamma}{\xi+\gamma}N(\xi) &= h''' + \frac{h''}{\xi+\gamma} - \frac{h'}{(\xi+\gamma)^2}\\ &+\frac{\gamma}{\xi+\gamma}\left[\left(\frac{m+1}{2}\right)hh'' - m(h')^2\right]\\ &-N_4^n\left[(n+1)h''' + \frac{(1-n)h''}{\xi+\gamma} + \frac{(n-1)h'}{(\xi+\gamma)^2}\right]\\ &-\frac{M^2\gamma^2 h'}{(\xi+\gamma)^2} + \frac{\gamma}{(\xi+\gamma)^2}\left(\frac{m+1}{2}\right)hh', \end{aligned} \quad (21)$$

subject to

$$\begin{aligned}&h(0)|_{\xi=0} = 0, h'(0)|_{\xi=0} = 1,\\ &h'(\infty)|_{\xi=\infty} = 0, h''(0)|_{\xi=\infty} = 0. \end{aligned} \quad (22)$$

In these equations, $M^2 = \frac{\sigma B_o^2 a^2}{\eta_0}$ represents the Hartmann number and $We = a^2\Gamma Re_s$ the Weissenberg number whereas $N_4 = We\left(h'' - \frac{h'}{\xi+\gamma}\right)$. In the limit of γ approaches infinity at $N = 0$, equations ($\forall m \geq 0$) of fluid flow past a flat surface is recovered and it substantiates the accuracy of present model.

$$h''' + \left(\frac{m+1}{2}\right)hh'' - m(h')^2 = (Weh'')^n(n+1)h''' - M^2h', \quad (23)$$

Utilizing Eq. (20) in Eq. (21), the pressure term varnishes and we get

$$\begin{aligned}&h'''' + \frac{2h'''}{\xi+\gamma} - \frac{h''}{(\xi+\gamma)^2} + \frac{h'}{(\xi+\gamma)^3}\\ &+\frac{\gamma}{\xi+\gamma}\left[\left(\frac{m+1}{2}\right)hh''' - \left(\frac{3m-1}{2}\right)h'h''\right]\\ &-\frac{\gamma}{(\xi+\gamma)^3}\left(\frac{m+1}{2}\right)hh' + \frac{\gamma}{(\xi+\gamma)^2}\left[\left(\frac{m+1}{2}\right)hh''\right.\\ &\left.-\left(\frac{3m-1}{2}\right)(h')^2\right] = N_4^n\left[(n+1)h'''' + \frac{h'''}{\xi+\gamma}\right.\\ &\left.+\frac{(n-1)h''}{(\xi+\gamma)^2} - \frac{(n-1)h'}{(\xi+\gamma)^3}\right] + \frac{nN_4^n}{\left(h'' - \frac{h'}{\xi+\gamma}\right)}\left[(n+1)(h''')^2\right.\\ &\left.-\frac{2nh''h'''}{\xi+\gamma} + \frac{2nh'h'''}{(\xi+\gamma)^2} + \frac{(n-1)(h'')^2}{(\xi+\gamma)^2}\right]\\ &-\frac{nN_4^n}{\left(h'' - \frac{h'}{\xi+\gamma}\right)}\left[\frac{(2n-2)h'h''}{(\xi+\gamma)^3} + \frac{(n-1)(h')^2}{(\xi+\gamma)^4}\right]\\ &+\frac{M^2\gamma^2}{(\xi+\gamma)^2}\left(h'' - \frac{h'}{\xi+\gamma}\right). \end{aligned} \quad (24)$$

4. Heat Transfer Analysis

Under the present flow conditions, the heat transport by virtue of energy equation follows

$$\rho C_p\frac{DT}{Dt} = \overline{\nabla}(K\overline{\nabla}T) + \Phi + \overline{\nabla}.\overline{q} + Q_o, \quad (25)$$

where $\Phi = 2\overline{S}(S_{rr}^2 + S_{rs}^2 + S_{ss}^2)$ is viscous dissipation term, $Q_o = \frac{1}{\sigma}(\bar{J}\times\bar{J})$ the ohmic heating term and C_p, T, K, and $\overline{q}$ represent fluid- heat capacity, temperature, thermal conductivity, and ohmic heating respectively.

By Rosseland expression, radiative flux $\bar{q}$ gives

$$\bar{q} = -\frac{4\sigma^*}{3\gamma^*}\frac{\partial T^4}{\partial r} \quad (26)$$

such that γ^*, σ^* are mean spectral absorption coefficient and Stefan-Boltzmann constant respectively. It worth nothing that for small heat kinetics, Eq. (26) can be linearized. However, this investigation is subjected to substantial high nonlinear radiation. The radiative heat flux is now expanded as

$$\bar{q} = -\frac{16\sigma^*}{3\gamma^*}T^3\frac{\partial T}{\partial r} \quad (27)$$

Incorporating Eq. (27) into Eq. (25), the temperature boundary layer region becomes

$$\begin{aligned}v\frac{\partial T}{\partial r} + \frac{Ru}{R+r}\frac{\partial T}{\partial s} &= \pi(1+RnT^3)\frac{\partial^2 T}{\partial r^2} + 3\pi RnT^2\left(\frac{\partial T}{\partial r}\right)^2\\ &+ \frac{\pi}{R+r}\frac{\partial T}{\partial r} + \frac{\sigma R^2 B_0^2 u^2}{\rho C_p(R+r)^2} + \frac{\frac{\eta_0}{\rho C_p}\left(\frac{\partial u}{\partial r} - \frac{u}{R+r}\right)^2}{1+\left[\Gamma\left(\frac{\partial u}{\partial r} - \frac{u}{R+r}\right)\right]^n}. \end{aligned} \quad (28)$$

$T \to T_\infty$ and $T = T_w$ referred as the ambient and surface temperature respectively whereas $\pi = \frac{K}{\rho C_p}$ denotes fluid thermal diffusivity and $Rn = \frac{16\sigma^*}{3\gamma^* K}$ being the radiation parameter.

Require boundary conditions

$$T(0)|_{r=0} = T_w(0) = 0, T(0)|_{r\to\infty} \to T_\infty. \quad (29)$$

Using an existing similarity quantity in non-dimensional form

$$\theta(\xi) = \frac{T - T_\infty}{T_w - T_\infty}, \quad (30)$$

Invoking Eqs. (17) - (19) and (30) in Eq. (28) we get

$$\begin{aligned}&\frac{(1+Rn)[1+(\theta_w-1)\theta]^3}{Pr}\theta''\\ &= \frac{3Rn(1-\theta_w)[1+(\theta_w-1)\theta]^2}{Pr}(\theta')^2 - \frac{\theta'}{Pr(\xi+\gamma)}\\ &-\frac{\gamma(m+1)h\theta'}{2(\xi+\gamma)} - \frac{Ec\left(h'' - \frac{h'}{\xi+\gamma}\right)^2}{1+\left[We\left(h'' - \frac{h'}{\xi+\gamma}\right)\right]^n}\\ &= \frac{\gamma^2 w(h')^2}{Pr(\gamma+\xi)^3} \end{aligned} \quad (31)$$

Corresponding boundary conditions become

$$\theta(0)|_{\xi=0} = 1, \theta(\infty)|_{\eta=\infty} = 0, \tag{32}$$

in which $Pr = \frac{\eta_0 C_p}{K}$, $\theta_w = \frac{T_w}{T_\infty}$, $Ec = \frac{U_\infty^2}{C_p(T_w - T_\infty)}$, $Rd = \frac{16\sigma^* T_\infty^3}{3k^* K_0}$, and $w = \frac{\sigma B_0^2 U_\infty^2 a^2}{K(T_w - T_\infty)}$ are known as Prandtl number, temperature parameter ($\theta_w \geq 1$), Eckert number, radiation parameter, and Ohmic heating parameter respectively. and $Br = PrEc$ the Brinkman number. It worth mentioning that radiative flux arises when $\theta_w > 1$.

In response to industrial significance of this work from engineering point of view, physical quantities such as surface drag force and rate of heat transfer are calculated as

$$C_{sk} = \frac{\tau_{rs}|_{r=0}}{\frac{1}{2}\rho u_w^2}, Nu = \frac{s\bar{q}}{K(T - T_w)}, \tag{33}$$

where $u_w = as^m$, $\tau_{rs}|_{r=0} = \frac{\eta_0\left(\frac{\partial u}{\partial r} - \frac{u}{R+r}\right)}{1+\left[\Gamma\left(\frac{\partial u}{\partial r} - \frac{u}{R+r}\right)\right]^n|_{r=0}}$, and $\bar{q} = -K\frac{\partial T}{\partial r}|_{r=0}$.

Utilizing this expression together with Eqs. (15)-(19) into Eq. (33), we obtain

$$-\frac{1}{2}R_{es}^{\frac{1}{2}} C_{sk} = \frac{h''(0) - \frac{1}{\gamma}}{1 + \left[We\left(h''(0) - \frac{1}{\gamma}\right)\right]^n} \tag{34}$$

and

$$R_{es}^{-\frac{1}{2}} Nu = -\theta'(0). \tag{35}$$

These equations are indispensable in thermal engineering and flow control.

5. Computations Approach

Analytic approach to solve the boundary value problems, BVPs obtained in Eqs. (24) and (31) subjected to Eqs. (22) and (32) remains a task and open for future investigation. This section presents a numerical method. Firstly, BVPs initializes into initial value problem, IVPs using

$$h = s_1, h' = s_2, h'' = s_3, h''' = s_4, \theta = s_5, \theta' = s_6, \tag{36}$$

After effecting Eq. (36), Eqs. (24) and (31) are linearised into first order of the form

$$\begin{pmatrix} s_1' \\ s_2' \\ s_3' \\ s_4' \\ s_5' \\ s_6' \end{pmatrix} = \begin{pmatrix} s_2 \\ s_3 \\ s_4 \\ -2\beta s_4 + \beta^2 s_3 - \beta^3 s_2 - \beta\gamma\left[\left(\frac{m+1}{2}\right) s_1 s_4 + \beta\gamma\left(\frac{3m-1}{2}\right) s_2 s_3\right] \\ -(We)^n (s_3 - \beta s_2)^n [(n+1)s_4' + \beta s_4 + (n-1)\beta^2 s_3 - (n-1)\beta^3 s_2] \\ -n(We)^n (s_3 - \beta s_2)^{n-1}[(n+1)s_4^2 - 2n\beta s_3 s_4 + 2n\beta^2 s_2 s_4 \\ +(n-1)\beta^2 s_3^2 - (2n-2)\beta^3 s_2 s_3 + (n-1)\beta^4 s_2^2] \\ +M^2\gamma^2\beta^2(s_3 - \beta s_2)s_6 \\ -\frac{1}{1+RnD_1^3}\left[\gamma\beta Pr\left(\frac{m+1}{2}\right) s_1 s_6 + 3Rn(\theta_w - 1)D_1^2 s_6^2 + \beta s_6\right] \\ -\frac{1}{1+RnD_1^3}\left(\frac{PrEc(s_3 - s_2)^2}{1+[We(s_3 - s_2)]^n} + w\gamma^2\beta^2 s_2^2\right) \end{pmatrix}, \tag{37}$$

subject to

$$\begin{pmatrix} s_1(0) \\ s_2(0) \\ s_3(0) \\ s_4(0) \\ s_5(0) \\ s_6(0) \end{pmatrix} = \begin{pmatrix} 0 \\ 1 \\ z_1 \\ z_2 \\ 1 \\ z_3 \end{pmatrix} \tag{38}$$

where $D_1 = 1 + (\theta_w - 1)\theta$ and $\beta = \frac{1}{\xi+\gamma}$ whereas z_1, z_2, and z_3 are initial missing conditions. Employing Keller-Box shooting technique together with Jacobi iterations [40]. Let

$$\begin{aligned} &w' = w_1, w_1' = w_2, w_2' = w_3, ..., w_{k-1}' \\ &= H(\xi, w_1, w_2, w_3, ..., w_{k-1}), \end{aligned} \tag{39}$$

$$\begin{aligned} \frac{w_i^{k+1} - w_{i-1}^k}{\delta h} &= (w_1)_{i-1/2}^k, \\ \frac{(w_1)_i^{k+1} - (w_1)_{i-1}^k}{\delta h} &= (w_2)_{i-1/2}^k, \\ &... \\ \frac{(w_{n-1})_i^{k+1} - (w_{n-1})_{i-1}^k}{\delta h} &= H_2(\xi_{i-1/2}^k, w_{i-1/2}^k, (w_1)_{i-1/2}^k, \\ &..., (w_{n-1})_{i-1/2}^k) \end{aligned} \tag{40}$$

Implementing Eq. (40) explicitly, we can write

$$\begin{aligned} &(\delta h)^{-1}(s_i^{k+1} - s_{i-1}^k) = -0.5((s_1)_i^k + (s_1)_{i-1}^k), \\ &s_0^{k+1} = 0, \\ &(\delta h)^{-1}((s_1)_i^{k+1} - (s_1)_{i-1}^k) = -0.5((s_2)_i^k + (s_2)_{i-1}^k), \\ &(s_1)_0^{k+1} = 1, \\ &(\delta h)^{-1}((s_2)_i^{k+1} - (s_2)_{i-1}^k) = -0.5((s_3)_i^k + (s_3)_{i-1}^k), \\ &(s_2)_0^{k+1} = z_1, \\ &(s_4)_i^{k+1} - (s_4)_{i-1}^k = -\delta h[2\beta((s_4)_i^k + (s_4)_{i-1}^k) \end{aligned}$$

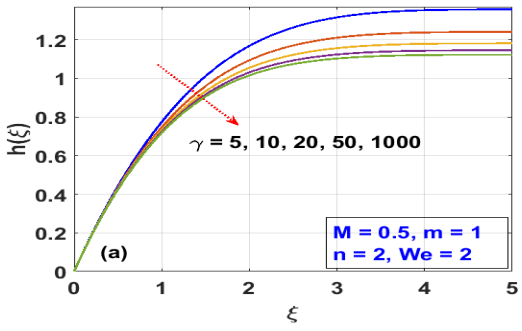


Figure 2: (a) to (e). Effects of γ, M, m, n, and We on $f(\xi)$

$$
\begin{aligned}
&-\beta^2((s_3)_i^k + (s_3)_{i-1}^k)] \\
&-\delta h[((s_3)_i^k + (s_3)_{i-1}^k) - \beta((s_2)_i^k + (s_2)_{i-1}^k)]^n A_1 \\
&-\delta h[((s_3)_i^k + (s_3)_{i-1}^k) - \beta((s_2)_i^k + (s_2)_{i-1}^k)]^{n-1} A_2 \\
&-\delta h\beta^3((s_2)_i^k + (s_2)_{i-1}^k) + \delta h M^2\gamma^2\beta^2 A_5 \\
&-\delta h\gamma\beta\left(\frac{m+1}{2}\right)A_3 + \delta h\gamma\beta\left(\frac{3m+1}{2}\right)A_4 \\
&(s_3)_0^{k+1} = z_2, \\
&(s_5)_i^{k+1} - (s_5)_{i-1}^k = -0.5\delta h((s_6)_i^k - (s_6)_{i-1}^k), \\
&(s_5)_0^{k+1} = 1, \\
&(s_6)_i^{k+1} - (s_6)_{i-1}^k = -\frac{\delta h}{1 + RnD_1^2}A_6, \\
&(s_6)_0^{k+1} = z_3,
\end{aligned}
$$

where z_i for $i = 1(1)3$ are missing initial conditions. These constants are randomly selected using MATLAB solver. Their choices of values are changed and the accuracy is determined with corresponding end point. The iterations loop with the step size ($\delta h = 0.01$) until the solutions are found satisfying the criterion $|\|w^{(n+1)}\|_2 - \|w^n\|_2| < \epsilon$.

6. Error Analysis

Theorem: Let $W_1 = W_1(h, h_1, h_2, h_3)$, and $W_2 = W_2(\theta, \theta_1, h, h_1, h_2)$ be differentiable functions, the maximum error reached by the Keller-Box shooting technique together with Jacobi iterations for Eq. (24) is bounded.

Proof:

Discretising this equation following the Keller-Box method with Jacobi iterative scheme, one can write

$$
\begin{aligned}
\frac{h_i^{n+1} - h_{i-1}^n}{\delta h} + (h_1)_{i-1/2}^n &= 0, \\
\frac{(h_1)_i^{n+1} - (h_1)_{i-1}^n}{\delta h} + (h_2)_{i-1/2}^n &= 0, \\
\frac{(h_2)_i^{n+1} - (h_2)_{i-1}^n}{\delta h} + (h_3)_{i-1/2}^n &= 0, \\
\frac{(h_3)_i^{n+1} - (h_3)_{i-1}^n}{\delta h} + (W_1)_{i-1/2}^n &= 0
\end{aligned} \tag{41}
$$

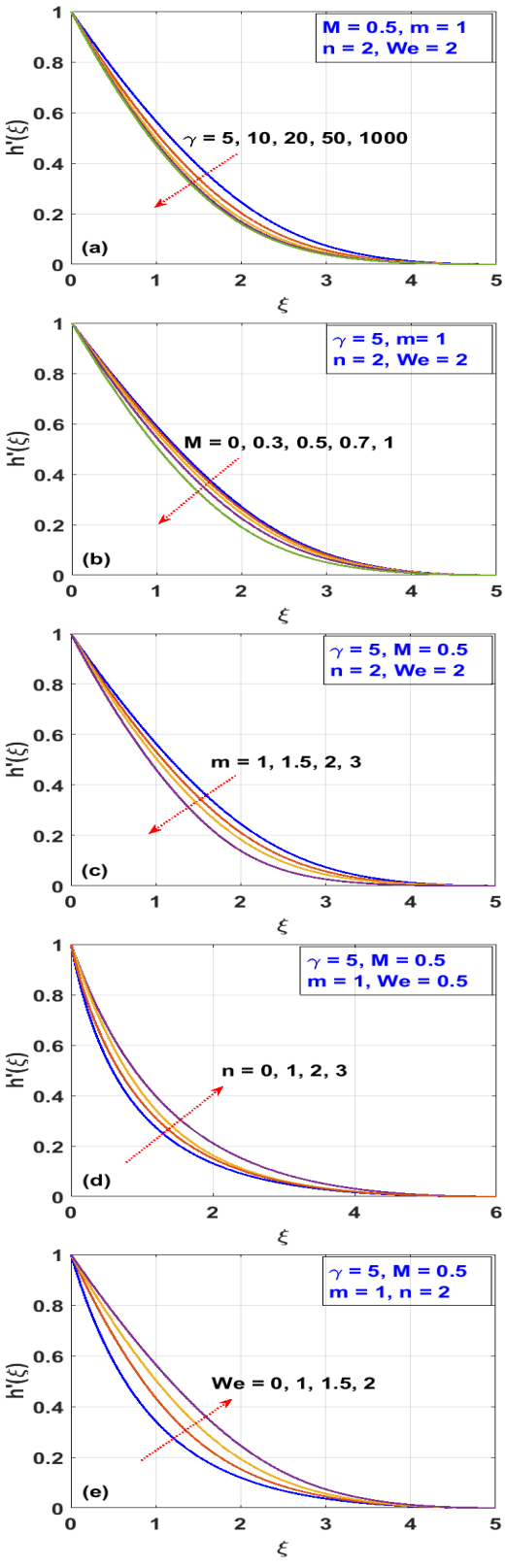


Figure 3: (a) to (e). Effects of γ, M, m, n, and We on $f'(\xi)$

in which the exact scheme can be written as

$$
\frac{h_i^E - h_{i-1}^E}{\delta h} + (h_1)_{i-1/2}^E = 0,
$$

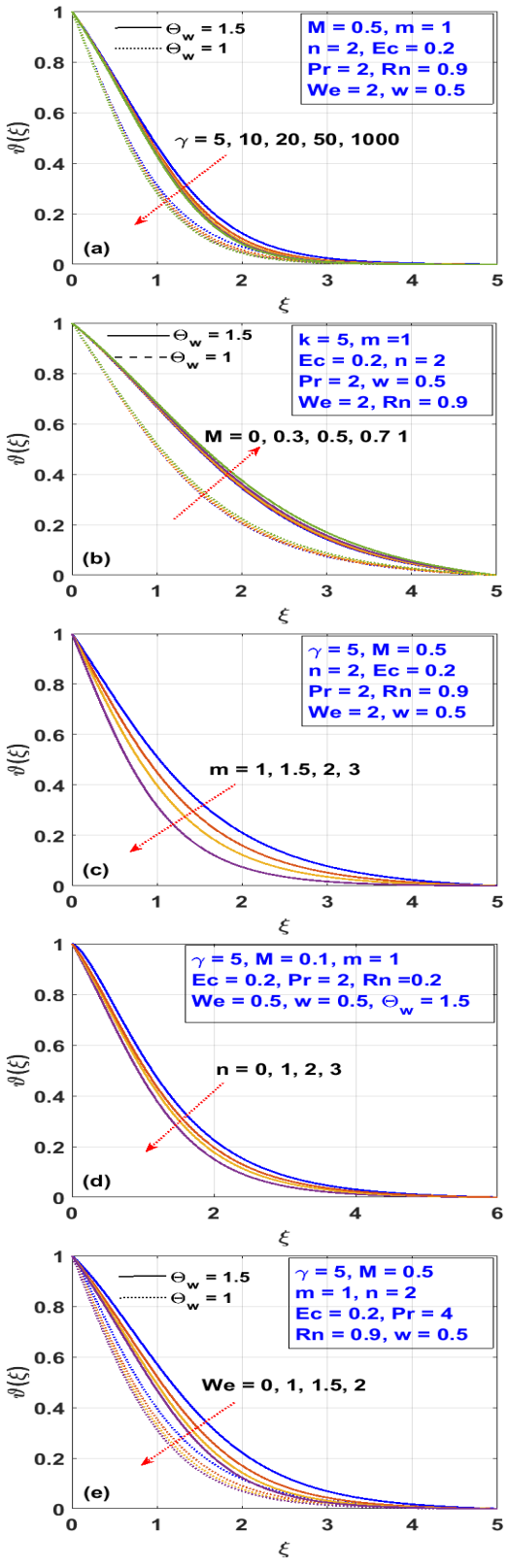


Figure 4: (a) to (e). Effects of γ, M, m, n, and We on $\theta(\xi)$

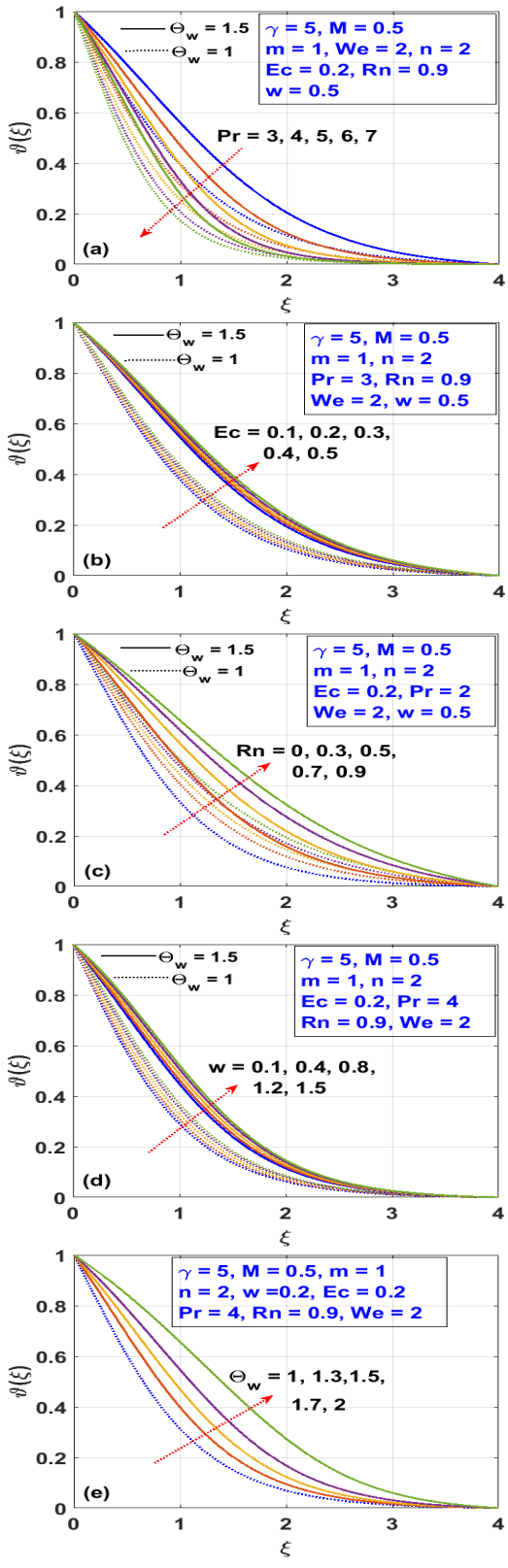


Figure 5: (a) to (e). Effects of Pr, Ec, Rn, w, and θ_w on $\theta(\xi)$

$$\frac{(h_1)_i^E - (h_1)_{i-1}^E}{\delta h} + (h_2)_{i-1/2}^E = 0,$$

$$\frac{(h_2)_i^E - (h_2)_{i-1}^E}{\delta h} + (h_3)_{i-1/2}^E = 0,$$

$$\frac{(h_3)_i^E - (h_3)_{i-1}^E}{\delta h} + (W_1)_{i-1/2}^n = 0, \quad (42)$$

subject to solution error at any grid point of the form

$$\begin{aligned}(e_1)_i^n &= h_1^n - h_1^E,\\ (e_2)_i^n &= (h_1)_i^n - (h_1)_i^E,\\ (e_3)_i^n &= (h_2)_i^n - (h_2)_i^E,\\ (e_4)_i^n &= (h_3)_i^n - (h_3)_i^E. \end{aligned} \quad (43)$$

By virtue of Mean Value Theorem, we get

$$\begin{aligned}W_1(h_i^n, (h_1)_i^n, (h_2)_i^n, (h_3)_i^n) - W_1(h_i^E, (h_1)_i^E, (h_2)_i^E, (h_3)_i^E)\\ = (\bar{e}_1)_i^n.\nabla W_1(z_1, z_2, z_3), \end{aligned} \quad (44)$$

in which

$$\begin{aligned}z_1 &= h_i^n + \varepsilon_1(h_2)_1^n,\\ z_2 &= (h_1)_i^n + \varepsilon_2(e_2)_i^n,\\ z_3 &= (h_2)_i^n + \varepsilon_3(e_3)_i^n, \end{aligned} \quad (45)$$

$z_i \epsilon [0, 1]$ for $i = 1(1)3$, and $(\bar{e}_1)_i^n = [(e_1)_i^n, (e_2)_i^n, (e_3)_i^n]$,

whereas convergence error equations are define as

$$\begin{aligned}(e_1)^{n+1} &= (e_1)_{i-1}^n + \delta h(e_1)_{i-1/2}^n,\\ (e_2)_i^{n+1} &= (e_2)_{i-1}^n + \delta h(e_2)_{i-1/2}^n,\\ (e_3)_i^{n+1} &= (e_3)_{i-1}^n + \delta h(\hat{e}_1)_{i-1/2}^n \nabla W_1, \end{aligned} \quad (46)$$

from Eq. (46), once can obtain the inequalities

$$\begin{aligned}|(e_1)_i^{n+1}| &\le |(e_1)_{i-1}^n| + \delta h|(e_2)_{i-1/2}^n|,\\ |(e_2)_i^{n+1}| &\le |(e_2)_{i-1}^n| + \delta h|(e_3)_{i-1/2}^n|,\\ |(e_3)_i^{n+1}| &\le |(e_3)_{i-1}^n| + \delta h|(\hat{e}_1)_{i-1/2}^n.\nabla W_1|. \end{aligned} \quad (47)$$

Setting $\nabla W_1 = [\bar{W}_1^1, \bar{W}_1^2, \bar{W}_1^3]$, Eq. (47) can be written as

$$\begin{aligned}|(e_3)_i^{n+1}| &\le |(e_3)_{i-1}^n| + \delta h|\Sigma_{j=1}^3 (e_j)_{i-1/2}^n \hat{W}_1^j|,\\ &\le |(e_3)_{i-1}^n| + \delta h\Sigma_{j=1}^3 |(e_j)_{i-1/2}^n \bar{W}_1^j|, \end{aligned} \quad (48)$$

such that

$$\begin{aligned}|(e_3)_i^{n+1}| &\le |(e_3)_{i-1}^n| + \delta h|\Sigma_{j=1}^3 (e_j)_{i-1/2}^n \hat{W}_1^j|,\\ &\le |(e_3)_{i-1}^n| + \delta h\Sigma_{j=1}^3 |(e_j)_{i-1/2}^n \bar{W}_1^j|. \end{aligned} \quad (49)$$

The maximum error is estimated in the form

$$\begin{aligned}(e_1)_i^n &= max_{i=1(1)N}|(e_1)_i^n|,\\ (e_2)_i^n &= max_{i=1(1)N}|(e_2)_i^n|,\\ (e_3)_i^n &= max_{i=1(1)N}|(e_3)_i^n|,\\ (\bar{e})^n &= max[max_{i=1(1)N}(e_1 = 1(1)N)_i^n], \end{aligned} \quad (50)$$

where N denotes the number of nodes and Eqs. (47) and (48) can be expressed as

$$\begin{aligned}e_1^{n+1} &\le e_1^n + \delta h e_2^n + \bar{M}_1 O(\delta h)^2,\\ e_2^{n+1} &\le e_2^n + \delta h e_3^n + \bar{M}_2 O(\delta h)^2,\\ \bar{e}^{n+1} &\le (1 + 4\delta h\Sigma_{j=1}^4 |\bar{W}_1^j|)\bar{e}^n + \bar{M}_3 O(\delta h)^2. \end{aligned} \quad (51)$$

Evaluating $n = 0, 1$, and n in the above expression, one can get

$$\begin{aligned}\bar{e}^1 &\le (1 + 4\delta h\Sigma_{j=1}^4 |\bar{W}_1^j|)\bar{e}^0 + \bar{M}_3 O(\delta h)^2,\\ &\bar{e}^2 \le (1 + 4\delta h\Sigma_{j=1}^4 |\bar{W}_1^j|)^2 \bar{e}^0\\ &+[1 + (1 + 4\delta h\Sigma_{j=1}^4 |\bar{W}_1^j|)]\bar{M}_3 O(\delta h)^2,\\ \bar{e}^n &\le (1 + 4\delta h\Sigma_{j=1}^4 |\bar{W}_1^j|)^n \bar{e}^0\\ &+[1 + (1 + 4\delta h\Sigma_{j=1}^4 |\bar{W}_1^j|) + ...,\\ &+(1 + 4\delta h\Sigma_{j=1}^4 |\bar{W}_1^j|)^{n-1}]\bar{M}_3 O(\delta h)^2. \end{aligned} \quad (52)$$

Taking nth term series sum, we obtain

$$\begin{aligned}\bar{e}^n &\le (1 + 4\delta h\Sigma_{j=1}^4 |\bar{W}_1^j|)^n \bar{e}^0\\ &+\left(\frac{[1 + 4\delta h\Sigma_{j=1}^4 |\bar{W}_1^j|]^n}{4\delta h\Sigma_{j=1}^4 |\bar{W}_1^j|}\right)\bar{M}_3 O(\delta h)^2,\\ &\le (1 + 4\delta h\Sigma_{j=1}^4 |\bar{W}_1^j|)^n \bar{e}^0\\ &+EXP(4\delta h\Sigma_{j=1}^4 |\bar{W}_1^j|)\bar{M}_3 O(\delta h)^2. \end{aligned} \quad (53)$$

Utilizing Eq. (53) into Eq. (52), one can get

$$\begin{aligned}e_1^n &\le (1 + \delta h)[(1 + 4\delta h\Sigma_{j=1}^4 |\bar{W}_1^j|)^n \bar{e}^0\\ &+EXP(4(n-1)\delta h\Sigma_{j=1}^4 |\bar{W}_1^j|)\bar{M}_3 O(\delta h)^2]\\ &+\bar{M}_1 O(\delta h)^2, \end{aligned} \quad (54)$$

$$\begin{aligned}e_2^n &\le (1 + \delta h)[(1 + 4\delta h\Sigma_{j=1}^4 |\bar{W}_1^j|)^n \bar{e}^0\\ &+EXP(4(n-1)\delta h\Sigma_{j=1}^4 |\bar{W}_1^j|)\bar{M}_3 O(\delta h)^2]\\ &+\bar{M}_2 O(\delta h)^2. \end{aligned} \quad (55)$$

Equations (54) and (55) express the maximum error bounds of Eqs. (22) and (24). In similar ways, maximum error can be obtained in view of Eqs. (31) and (32) (see ref. [40]).

7. Results and Graphical Analysis

This section presents the graphical illustrations of the flow quantities that is; the stream function $h(\xi)$, velocity $h'(\xi)$, and temperature $\theta(\xi)$ against characterizing parameters. Figures 2(a, b, and c) show the behaviour of stream function in response to curvature parameter γ, magnetic field M, and nonlinear stretching power m.

In these graphs, the stream function decreases for increasing these parameters which means that the flow trajectory can be minimized either by reducing the curvature or enhancing the Lorentz force as well as stretching power. On the other hand, in Figs. 2(d and e) the flow trajectory is enhanced by increasing the rheology parameters (n and We) of the fluid. This means that fluid resistance to flow reduces and the fluid behaves more likely as shear thinning. Figure 3(a) shows that the velocity $h'(\xi)$ decreases steadily by increasing radius of curvature (as the surface becomes flat). The velocity graphs plotted in Figs. 3(b and c) elucidate reductions in flow velocity as a consequence of opposing Lorentz force due to applied high magnetic field. This observation substantiates the impact of the Lorentz force and

Table 1: Comparison of Nusselt number, $-\theta'(0)$ with published results

Pr	Hammad [17]	Wang [18]	Khan *et al.* [12]	G and S [21]	Ijaz *et al.* [14]	Present Results
0.2	0.139100	0.169100	0.164037	0.139100	0.196550	0.196502
0.7	0.453900	0.453900	0.418299	0.453900	0.454446	0.454369
20	3.353900	3.353900	3.256030	3.353900	3.359500	3.353902
70	6.462200	6.462200	6.366620	6.462200	6.462290	6.462200

Table 2: Numerical values of the skin-friction coefficient and rate of heat transfer for $n = 2$.

Parameters									$\theta_w = 1$	$\theta_w = 1.5$
γ	M	m	Ec	Pr	Rn	We	w	$Re_s^{0.5}C_{sk}$	$-\theta(0)$	$-\theta(0)$
5	0.3	0	0.2	2	0.9	2	0.5	0.24141	0.48065	0.26879
-	0.4	-	-	-	-	-	-	0.24029	0.47929	0.26750
-	0.5	-	-	-	-	-	-	0.23888	0.47758	0.26590
-	-	1	-	-	-	-	-	0.22868	0.66205	0.25535
-	-	2	-	-	-	-	-	0.21036	0.82918	0.22628
10	-	0	0.1	-	-	-	-	0.24128	0.50082	0.28532
-	-	-	0.2	-	-	-	-	-	0.48188	0.27561
-	-	-	0.3	-	-	-	-	-	0.46295	0.26590
-	-	-	0.2	-	-	-	-	-	0.48188	0.33336
-	-	-	-	3	-	-	-	-	0.46474	0.38631
5	-	-	-	2	0.5	-	-	0.23888	0.55891	0.35957
-	-	-	-	-	0.7	-	-	-	0.51446	0.30477
-	-	-	-	-	-	1	-	0.49760	0.41772	0.22763
-	-	-	-	-	-	1.5	-	0.32994	0.45326	0.24932
10	-	-	-	-	-	-	0.5	0.24128	0.48188	0.27561
-	-	-	-	-	-	-	1.5	-	0.20253	0.13530
-	-	-	-	-	-	-	2	-	0.06285	0.06495

stretching power m and confirms the above conclusion made for the flow trajectory. In other words, the flow velocity can be regulated with the aid of geometry parameters that is radius of curvature, magnetic field, and stretching power. To investigate the rheology effects n- fluid power-law behavior and We-Weissenberg number, figures 3(d and e) are plotted.

In these figures, the velocity increases for increasing n and We. Physically, shear thinning (low viscosity) of the fluid shows less resistance to flow and invariably enlarges the momentum boundary-layer. Figure 4 is given to illustrates the influence of nonlinear radiation $\theta_w > 1$ on temperature profile as compared to linear radiation $\theta_w = 1$. In Fig. 4(a), we observe that increasing radius of curvature γ decreases the temperature profile $\theta(\xi)$ as well as thermal boundary layer region. This observation on the other hand shows that, heat flows more quickly over curved surface which can be controlled by value of γ. A striking difference is obvious when $\theta_w = 1.5$ as compared with $\theta_w = 1$. Effect of increasing magnetic field on temperature is displayed in Fig. 4(b). The thermal characteristics is increased due to opposing Lorentz force. A usual contribution in thermal engineering study with reason being that the force induced heat from the curved surface to the fluid. The effect of stretching power on temperature profile is plotted in Fig. 4(c). This graph shows that increasing m shrinks the thermal region as well as associated thermal boundary layer. This observation infers that either any side of the thermal spectrum can also be controlled by virtue of stretching power of the fluid velocity.

Figures 4(d and e) elucidate the impacts of fluid parameters (n and We) on temperature profile. In both graphs, the thermal kinetic energy decreases for large fluid power-index and Weissenberg number. This observation implies that shear thinning fluid absorbed more heat due to weak or free viscous bond. Figure 5 maintains the usual interpretations of the various physical parameters involved in this problem. Figure 5(a) shows a decrease in temperature profile as a consequence of lowering thermal conductivity of the fluid for large Pr. Figure 5(b) indicates a positive response of viscous heating in enhancing the thermal energy of the fluid by increasing Ec. This observation is more significant when $\theta_w = 1.5$. The effect of radiation on temperature profile is given in Fig. 5(c). As habitual source of

heat, increasing Rn enlarges the thermal boundary layer thickness and temperature profile. The effect of Ohmic heating from surface to the temperature field is given in Fig. 5(d).

In this graph, the thermal characteristics increase slightly for increasing w due to additional heat generated at the surface to the fluid and invariably enhances fluid temperature. Finally, the impact of temperature difference on temperature as well as thermal boundary layer thickness is substantiated in Fig. 5(e) showing a positive influence of nonlinear radiation. In other words, increasing temperature difference θ_w parameter expands the temperature and associated boundary thickness. Table 1 compares the present results of heat transfer with published work in the limiting case when $n = 0$, $Rn = 0$, $M = 0$, $w = 0$, $Ec = 0$, and $We = 0$. It can be seen that the results in the literature are special cases of the present study. Table 2 presents the impact of various parameters on the skin friction coefficient and rate of heat transfer for the present problem.

8. Concluding Remark

Modelling of nonlinear radiative heat transfer of an electrically conducting Cross-fluid under variable applied magnetic field has been studied. Governing equation is conducted in the presence of viscous dissipation and Ohmic heating. The fluid motion is induced by power-law stretching velocity over curved surface mechanism.The behaviours of flow field- velocity as well as temperature against interesting parameters are summarized.

1. The flow stream patterns, velocity, and associated boundary-layer thickness are increased for large number of fluid rheology n and Weissenberg number We. Opposite effects are observed for increasing geometry curvature γ, magnetic field M, and stretching power m. That is, the flow stream together with the velocity and associated boundary-layer thickness are decreased.

2. The temperature profile together with thermal boundary-layer are reduced for large curvature and stretching power.

3. Increase in magnetic field enhances the thermal region and consequently enlarges its thermal boundary-layer.

4. Existing interpretation of thermal profiles for Eckert number Ec, Prandtl number Pr, radiation Rn parameter, and Ohmic heating parameter w, are well established.

5. The present work is comparatively substantiated by the impact of nonlinear radiation through temperature difference θ_w parameter. Therefore, profound results are well recorded in both linear and nonlinear radiations.

6. The practical significance of the present results is that, the flow as well as heat transfer phenomena can be controlled, maintained, and optimized through various studied parameters. Thus, theses results obtained are useful in polymer dynamics of stretchable materials and curved mechanism.

References

[1] T. Hayat, M. Zubair, M. Ayub, M. Waqas & A. Alsaedi, " Stagnation point flow towards nonlinear stretching surface with Cattaneo-Christov heat flux", Eur Phys J Plus **131** (2016) 355.

[2] B.C. Rout & S. R. Mishra, " Thermal energy transport on MHD nanofluid flow over a stretching surface: A comparative study", Eng Sci Tech Int J **21(1)** (2018) 69.

[3] M. Turkyilmazoglu "Flow of a micropolar fluid due to a porous stretching sheet and heat transfer", Int J Nonlinear Mech **83** (2016) 64.

[4] A. Zeeshan, A. Majeed & R Ellahi, "Effect of magnetic dipole on viscous ferro-fluid past a stretching surface with thermal radiation", J Mol Liq **215** (2016) 554.

[5] R. Mohamed, M. L. Eid Kasseb, T. Mohammed & M. Sheikholeslami, "Numerical treatment for Carreau nanofluid flow over a porous nonlinear stretching surface", Results Phys **8** (2018) 1193.

[6] B.C. Prasannakumara, B. J. Gireesha, M. R. Krishnamurthy & K. G. Kumar, "MHD flow and nonlinear radiative heat transfer of Sisko nanofluid over a nonlinear stretching sheet", Inf Med Unlocked **9** (2017) 132.

[7] A. S. Feroz, M. Usman, R. Ul Haq & W. Wang, "Melting heat transfer analysis of Sisko fluid over a moving surface with nonlinear thermal radiation via collocation method", Heat Mass Transfer **126** (2018) 1042.

[8] L. A. Lund, Z. Omar & K llyas, "Analysis of dual solution for MHD flow of Williamson fluid with Slippage", Heliyon **5(3)** (2019) 20.

[9] R. Khalil, A. Qaiser, M. Y. Malik & U. Ali, "Numerical communication for MHD thermally stratified dual convection flow of Casson fluid yields by stretching cylinder", Chinese J Phys **55(4)** (2017) 1614.

[10] A. Mohamed & A. A. Afify "Lie group analysis of hydromagnetic flow and heat transfer of a power-law fluid over stretching surface with temperature-dependent viscosity and thermal conductivity", Int J Mod Phys **27(11)** (2016) 20.

[11] T. Hayat, M. K. Ijaz, M. Tamoor, M. Waqas & A. Alsaedi "Numerical Simulation of heat transfer in MHD Stagnation point flow of Cross fluid model towards a stretched surface", Results Phys **7** (2017) 1827.

[12] M. Khan, M. Manzur & M. Rahman, "On axisymmetric flow and heat transfer of Cross fluid over a radially stretching sheet", Results Phys **7** (2017) 3772.

[13] M. Manzur, M. Khan & M. Rahman, "Mixed convection heat transfer to Cross fluid with thermal radiation: Effects of buoyancy assisting and opposing flows", Int J Mechanical Sci **139** (2018) 523.

[14] M. K. Ijaz, W. Waqas, T. Hayat & A. Alsaedi, "Magneto-hydrodynamical numerical simulation of heat transfer in MHD stagnation point flow of Cross fluid model towards a stretched surface", Phys Chem Liq **56(5)** (2017) 595.

[15] I-C. Liu, "Flow and heat transfer of an electrically conducting fluid of second grade in a porous medium over a stretching sheet subject to a transverse magnetic field", Int. J. Nonlinear Mech **40** (2005) 474.

[16] T. Hayat, A. Shafiq & A. Alsaedi, "Effect of Joule Heating and Thermal Radiation in flow of third grade Fluid over Radiative surface", PLoS ONE **9(1)** (2014) 153.

[17] A. A. Hamad, "Analytical solution of natural convection flow of a nanofluid over a linearly stretching sheet in the presence of magnetic field", Int Commun Heat Mass **38** (4)(2011) 492.

[18] A. B. Disu & S. O. Salawu, "Thermal distribution of magneto-tangent hyperbolic flowing fluid over a porous moving sheet: A lie group analysis", J. Nig. Soc. Phys. Sci. **5** (2023) 1103.

[19] P. B. Sharma, M. Kapalta, A. Kumar, D. Bains, S. Gupta & P. Thakur, "Electrodynamic Convection Dieletric Rotating Oldroydian Nanofluid in Porous Medium",J Nig Soc Phys Sci **5** (2023) 1137.

[20] C. Y. Wang, "Free convection on a vertical stretching surface", J Appl Math Mech **9** (1989) 420.

[21] R. S. R. Gorla & R. I. Sidawi, "Free convection on a vertical stretching surface with suction and blowing", Appl Sci Res **52** (1994) 257.

[22] M. Jalil & S. Asghar, "Flow of power-law fluid over a stretching surface: A Lie group analysis", Int J Nonlinear Mech **48** (2018) 71.

[23] M. Mustafa, J. A. Khan, T. Hayat & A. Alsaedi, "Simulation for Maxwell fluid flow past a convectively heated exponentially stretching sheet with nanoparticles", AIP Adv **5(3)** (2015) 133.

[24] M. Khan, R. Malik, A. Munir & W.A. Khan, "Flow and heat transfer in Sisko fluid with convective boundary conditions", PLoS ONE **9(10)** (2014) 989.

[25] T. Hayat, M. Farooq, A. Alsaedi & Z. Iqbal, "Melting heat transfer in the stagnation point flow of Powell-Eyring fluid", J Thermophys Heat **27** (2013) 766.
[26] E. Azhar, Z. Iqbal, S. Ijaz, & E. N. Maraj, "Numerical approach for stagnation point flow of Sutterby fluid impinging to Cattaneo-Christov heat flux model", Pramana – J Phys **91** (2018) 61.
[27] M. Sajid, N. Ali, T. Javed & Z. Abbas, "Stretching a curved surface in a viscous fluid", Chinese Phys Lett **27** (2010) 703.
[28] Z. Abbas, M. Naveed & M. Sajid, "Heat transfer analysis for stretching flow over a curved surface with magnetic field", J Eng Thermophys **22** (2013) 345.
[29] K. M. Sanni, Q. Hussain & S. Asghar, "Heat transfer analysis for nonlinear boundary driven flow over a curved stretching sheet with a variable magnetic field", Front Phys **8** (2020) 113.
[30] K. M. Sanni, Q. Hussain & S. Asghar, "Thermal Analysis of a Hydromagnetic Viscoelastic Fluid Over a Continuous Curved Stretching Surface in the Presence of Radiative Heat Flux", Arab J Sci Eng **2020** 2020 8.
[31] F. Saba, N. Ahmed, S. Hussain, U. Khan & S. T. Mohyd-Din, "Thermal Analysis of Nanofluid Flow over a Curved Stretching Surface Suspended by Carbon Nanotubes with Internal Heat Generation", Appl Sci **8** (2018) 395.
[32] T. Hayat, R. Sajjad, R. Ellahi, A. Alsaedi & T. Muhammad, "Homogeneous-heterogeneous reaction in MHD flow of Micropolar fluid by a Curved Stretching Surface", J Mol Liq **240** (2017) 220.
[33] S. H. Saleh, M. Arfin, R. Nazar & I. Pop, "Unsteady Micropolar Fluid over a Permeable Curved Stretching Shrinking Surface", Math Probl Eng **2017** (2017) 13.
[34] M. Naveed, Z. Abbas & M. Sajid, "Dual Solutions in Hydromagnetic Viscous Fluid Flow Past a Shrinking Curved Surface", Arab J Sci Eng **43** (2018) 1194.
[35] K.M. Sanni, S. Asghar, M. Jalil & N. F. Okechi, "Flow of viscous fluid along a nonlinearly stretching curved surface", Results Phys **7** (2017) 7.
[36] S. Nadeem, Z. Ahmed & S. Saleem, "Carbon nanotubes effect in magneto nanofluid flow over a curved stretching surface with variable viscosity, Microsyst Technol", **25** (2018) 2888.
[37] M. M. Cross, "Rheology of non-Newtonian fluids: A new flow equation for pseudoplastic systems", J Colloid Sci **20(5)** (1965) 437.
[38] K. M. Sanni, Q. Hussain & S. Asghar, "Heat transfer analysis for nonlinear boundary driven flow over a curved stretching sheet with a variable magnetic field", Front Phys **8** (2020) 113.
[39] K. M. Sanni, Q. Hussain & S. Asghar, "Thermal Analysis of a Hydromagnetic Viscoelastic Fluid Over a Continuous Curved Stretching Surface in the Presence of Radiative Heat Flux", Arab J Sci Eng **2020** (2020) 8.
[40] Yasir N & Shoaib Arif M, "Keller-Box shooting method and its application to nanofluid flow over convectively heated sheet with stability and convergence. Num Heat Transfer, B: Fundamentals", **76** (2019) 180.

9. APPENDIX

$$
\begin{aligned}
A_1 &= (We)^n\left((n+1)\frac{(s_4)_i^{k+1}-(s_4)_{i-1}^k}{\delta h}+\beta((s_4)_i^k+(s_4)_{i-1}^k)\right)\\
&+ (We)^n(n-1)\beta^2((s_3)_i^k+(s_3)_{i-1}^k)\\
&- (We)^n(n-1)\beta^3((s_2)_i^k+(s_2)_{i-1}^k)\\
A_2 &= n(We)^n(n+1)((s_4)_i^k+(s_4)_{i-1}^k)^2\\
&- 2n^2\beta(We)^n((s_3)_i^k+(s_3)_{i-1}^k)((s_4)_i^k+(s_4)_{i-1}^k)\\
&+ 2n^2\beta^2(We)^n((s_2)_i^k+(s_2)_{i-1}^k)((s_4)_i^k+(s_4)_{i-1}^k)\\
&+ n(n-1)(We)^n\beta^2((s_3)_i^k+(s_3)_{i-1}^k)^2\\
&- n(2n-2)(We)^n\beta^3((s_2)_i^k+(s_2)_{i-1}^k)((s_3)_i^k+(s_3)_{i-1}^k)\\
&+ (n-1)\beta^4((s_2)_i^k+(s_2)_{i-1}^k)\\
A_3 &= ((s_1)_i^k+(s_1)_{i-1}^k)((s_4)_i^k+(s_4)_{i-1}^k)\\
A_4 &= ((s_2)_i^k+(s_2)_{i-1}^k)((s_3)_i^k+(s_3)_{i-1}^k)\\
A_5 &= (((s_3)_i^k+(s_3)_{i-1}^k)-\beta((s_2)_i^k+(s_2)_{i-1}^k))\\
A_6 &= \gamma\beta Pr\left(\frac{m+1}{2}\right)((s_1)_i^k+(s_1)_{i-1}^k)((s_6)_i^k+(s_6)_{i-1}^k)\\
&+ 3Rn(\theta_w-1)D_1^2((s_6)_i^k+(s_6)_{i-1}^k)^2+\beta((s_6)_i^k+(s_6)_{i-1}^k)\\
&+ \frac{PrEc(((s_3)_i^k+(s_3)_{i-1}^k)-\beta((s_2)_i^k+(s_2)_{i-1}^k))^2}{1+[We(((s_3)_i^k+(s_3)_{i-1}^k)-\beta((s_2)_i^k+(s_2)_{i-1}^k))]^n}\\
&+ w\gamma^2\beta^2((s_2)_i^k+(s_2)_{i-1}^k)^2
\end{aligned}
$$